Check for updates

Extraction of high-quality grade cellulose and cellulose nanocrystals from different lignocellulosic agri-food wastes

Cesare Rovera[1], Daniele Carullo[1], Tommaso Bellesia[1], Duygu Büyüktaş[1], Masoud Ghaani[1], Enrico Caneva[2] and Stefano Farris[1,3]*

[1]Food Packaging Lab, Department of Food, Environmental and Nutritional Sciences (DeFENS), University of Milan, Milan, Italy, [2]Comprehensive Substances Characterization via Advanced Spectroscopy Technology Platform, University of Milan (UNITECH COSPECT), Milan, Italy, [3]INSTM, National Consortium of Materials Science and Technology, Local Unit University of Milan, Milan, Italy

Introduction: Prompted by the increasing need for an intensified valorization of agri-food waste, in this work a three-step chemical procedure was used to extract high-purity cellulose from garlic stalk, corncob, and giant cane cut-up by a sequential removal of hemicellulose, lignin, ash, and organic compounds. Cellulose nanocrystals of potential interest for nanocomposite applications were then obtained through acid hydrolysis.

Methods: The purity of the cellulose was determined employing Nuclear Magnetic Resonance and infrared spectroscopy, whereas dynamic light scattering, optical, atomic force microscopy, and transmission electron microscopy were used for morphological characterization. The high purity and crystallinity of cellulose was confirmed by comparison with the ultra-pure bacterial cellulose originating from *K. sucrofermentans*, irrespective of the waste used.

Results and discussion: At the end of the extraction procedure, cellulose yields of 35.73, 37.15, and 39.10%, for garlic stalk, corncob, and giant cane cut-up, respectively, were achieved. Dynamic light scattering and atomic force microscopy analyses showed that the length of the whisker-like nanocrystals depended on the raw material (from ∼100 nm up to > 2μm), while the final yield was ∼40−50% for all three wastes. The versatility and effectiveness of the method here proposed can be profitably used for a wide range of agro-waste feedstocks.

1. Introduction

In the last decades, the management of agro-waste feedstocks, especially of lignocellulosic origin, has increasingly become a relevant concern, together with the importance of their end-life options. As reported by McKendry (2002) and Sims (2003), lignocellulosic wastes encompass a large fraction of municipal solid waste, crop

residues, animal manure, woodlot arisings, forest residues, and dedicated energy crops. Therefore, such biomasses stand out as the most available feedstocks for the prospective development of a sustainable chemical and energy industry worldwide (Liguoria and Faraco, 2016).

Crop residues, in particular, can profitably be exploited to obtain high-added value materials after the efficient recovery of e.g., cellulose, hemicellulose, lignin, or several inorganic compounds. These materials can then be used for multiple industrial sectors, especially in the form of reinforcing fillers (Sjöström, 1993). Cellulose, in particular, frequently represents the largest fiber fraction amongst lignocellulosic wastes (40 to 50% by weight of the original biomass), whereas the concentration of hemicellulose and lignin varies largely as a function of the specific crop (McKendry, 2002; Peguero et al., 2022). Together with its functional properties, this is the main reason why the extraction of cellulose has attracted a great deal of attention within recent years at both academic and industrial levels (Reddy and Yang, 2005). Indeed, cellulose from agro-waste feedstocks can potentially find application in energy, water treatment, biomedical, food additives, and packaging industries (Azeredo et al., 2019; Abdul Khalil et al., 2020; Ganguly et al., 2020), both in its native form (Jayaramudu et al., 2013; Mondal et al., 2015; Reddy and Rhim, 2018; Moreno et al., 2019) and in its derivatives, such as micro-fibrillated cellulose (MFC) and cellulose nanocrystals (CNCs) (Chen et al., 2012; Rahman and Netraval, 2016). Not only the relative proportion between cellulose, hemicellulose, and lignin, but also the availability of the agro-waste feedstock (tons/year) must be considered to define the feasibility and sustainability of the whole valorization process of lignocellulosic waste. Accordingly, several agricultural wastes and by-products deriving from domestic or field-crop residues disclose a high potential for the development of new sources of cellulose (Reddy and Yang, 2005). In this work, we have decided to consider three different species as raw materials for cellulose extraction.

Garlic (*Allium sativum*) is currently the second most important species of the *Allium* genus worldwide, followed by onion, with an average planted surface area of about 1.5 million ha (FAOSTAT, 2016; Moreno et al., 2019). During harvesting and processing operations, up to 25–30% wt. of the total raw material, mainly represented by stalks and skills, is discarded as a waste (Kallel and Ellouz Chaabouni, 2017). Because garlic stalks and skill fractions are mainly composed of cellulose (41–50% dry weight biomass, DW_b), garlic has a great potential for the profitable extraction of cellulose (Reddy and Rhim, 2018).

Corn (*Zea Maize L.*) is the most important crop at a global level in terms of annual production (Shiferaw et al., 2011). In 2015, corn production in the United States exceeded 250 million tons (USDA-NASS, 2016; Méndez-Hernández et al., 2019). The interest in corn residues lies in the fact that for every 100 kg of corn grain obtained, ∼18 kg are represented by corncobs, which mostly remain unused as lignocellulosic waste (Torre et al., 2008; Lau et al., 2019). In recent years, corncob has been proven for

successful usage as a substrate to produce bioethanol, bio-oil, biochar, solid biofuel, xylooligosaccharides, and, more recently, fibers for the generation of nanocomposites (Yang et al., 2005; Chen et al., 2007; Ioannidou et al., 2009; Mullen et al., 2010; Silvério et al., 2013).

Not only agri-food waste but lignocellulosic feedstocks that do not compete with the food sector have also been used to obtain cellulose. For example, crops able to grow in marginal lands might open unprecedented perspectives, such as the possibility of valorizing the entire aerial biomass area while obtaining added-value products (Thomsen, 2005; Cherubini and Jungmeier, 2010; Calvo et al., 2018). *Arundo donax L.*, commonly known as giant cane or giant reed, is a non-food crop belonging to the *Poaceae* family. It is a perennial herbaceous, hydrophyte plant able to grow spontaneously in different kinds of marginal environments, under extreme conditions of water availability, and in all types of soils, ranging from heavy clay to lose or graveling sand (Ceotto and Di Candilo, 2010). For this reason, *A. donax* is widespread in temperate as well as in hot zones all over the world (Corno et al., 2014). The limited investment and the low maintenance costs deriving from agronomic intervention, low water, and fertilizer requirements (Corno et al., 2016), make this crop a suitable candidate for feeding a biorefinery process (Calvo et al., 2018).

One of the key aspects in the valorization of lignocellulosic agro-waste feedstock and by-products is linked to the extraction and purification procedures used to obtain cellulose. These procedures can have a great impact on the efficiency of the overall process in terms of time needed, costs, environmental impact, and yield. To date, several protocols have been reported, such as those based on strong acids/alkali hydrolytic treatments (Silvério et al., 2013; Reddy and Rhim, 2018; Hafemann et al., 2019). Despite their high purification yields, the above-mentioned techniques suffer from several drawbacks, such as the need for high-concentrated chemicals and long processing times, which unavoidably lead to increased energy requirements. Therefore, to overcome these shortcomings while providing enhanced process yields, it is of utmost importance to develop a fast, simple, tunable, and soft chemicals-required extractive process for cellulose purification from lignocellulosic agro-waste.

In this work, we propose a standardized cascaded chemical purification process to obtain cellulose from three different cellulose-rich lignocellulosic biomasses—garlic stalk, maize corncob, and giant cane cut-up. From the obtained high-purity cellulose, CNCs were finally extracted by acid hydrolysis and then characterized to envisage any possible application as fillers for nanocomposite systems, e.g., nanocomposite polymeric materials for food packaging applications. The novelty of this work lies in the versatility of the fast and easy procedure that we propose to extract efficiently high-purity cellulose from different agri-food wastes. In particular, we demonstrate that the same procedure can be used to obtain cellulose from garlic stalk, corncob, and giant cane cut up, according to

a cascade protocol. Cellulose nanocrystals (CNCs) from the above-mentioned biomasses can then be produced *via* acid hydrolysis. This approach totally fits with the circular economy principles, insomuch as a high added value product is recovered from food wastes and agricultural feedstocks to be possibly used, either in its native form or in its derivatives (CNCs), for different applications, e.g., for the food packaging industrial sector.

2. Materials and methods

2.1. Raw materials and chemicals

Corncob and giant cane cut-up were obtained from the experimental farm 'A. Menozzi' of the University of Milan (Landriano, Italy) (Calvo et al., 2018). These lignocellulosic wastes were first air-dried at 60°C (Memmert UF110plus, Schwabach, Germany) and then stored at 23.0 ± 0.5°C in a desiccator containing calcium chloride for 2 days before further processing. Garlic stalks (*Allium sativum*) were directly placed in a desiccator without any pretreatment. All lignocellulosic agro-wastes were then subjected to grinding using an M20 Universal mill (IKA®-Werke GmbH & Co., Staufen, Germany) provided with a double-walled grinding chamber for internal cooling, at a fixed speed of 20,000 rpm for 10 min. To select the smaller fractions of milled agro-wastes, a 70-mesh metal sieve (particle size retention: >210 μm) was used. The dry-sieved powder was kept at 23.0 ± 0.5°C in a desiccator for 2 days before chemical extraction. All the adopted chemicals (VWR International S.r.l., Milan, Italy) were of reagent grade and used without further purification. For each lignocellulosic feedstock, the initial composition was drawn from the literature and is reported in Table 1.

2.2. Extraction of cellulose from lignocellulosic agri-food wastes

The recovery of cellulose from lignocellulosic agro-wastes followed the extraction protocol used in previous works (Mondal and Haque, 2007; Mondal et al., 2015) with slight modifications intended to optimize each purification step (Figure 1). In the beginning, 2 g of lignocellulosic agro-wastes powder were dispersed into a 20% NaOH solution (w/v) at a solid-to-liquid ratio (S/L) of 1:100 (g/mL). The obtained mixture was kept under stirring at 300 rpm for 120 min (garlic stalks, and giant cane cut-up) or 180 min (corncob), at room temperature. The longer contact time adopted for corncob arose from the high abundancy of hemicellulose in the biomass (Table 1), thus requiring more severe conditions.

At the end of this first stage, the solid/liquid separation was achieved by means of a Büchner filtration setup using grade 230 Whatman® filter paper (particles retention: 20–30 μm,

Merck KGaA, Darmstadt, Germany). The solid residue was then washed thoroughly with 2% (v/v) acetic acid and hot distilled water (70°C) until the effluent became clear. The subsequent removal of the organic compounds was performed using pure xylene (S/L = 1:25 g/mL) under stirring at 500 rpm for 20 min at room temperature, followed by a washing step with technical-grade ethanol and subsequent filtration. As the last step, a 1% (w/v) $NaClO_2$ solution (S/L = 1:50 g/mL) buffered at pH 4 was used at 90°C and 500 rpm for 90 min (garlic stalks and giant cane cut-up) and 60 min (corncob) as both bleaching agent and to allow the removal of lignin residues possibly still present in the biomass.

At last, the so obtained cellulose was separated by filtering and washing using technical-grade ethanol and distilled water, and then air-dried at 60°C overnight before undergoing further characterization.

2.3. Production of macro-sized bacterial cellulose (BC)

BC was used in this study for comparison purposes, that is, as a reference substrate to be compared with the cellulose extracted from the three different lignocellulosic biomasses. The production of BC followed the same procedure as described in our previous work (Rovera et al., 2018). Briefly, BC was synthesized by static fermentation (7 days at 30°C in a Hestrin and Schramm culture medium) using the *Komagataeibacter sucrofermentans* DSM 15973 strain (Leibniz Institute DSMZ-German Collection of Microorganisms and Cell Cultures, Braunschweig, Germany). BC pellicles were washed with deionized water and boiled in an alkaline solution (NaOH, 1M) for 30 min to remove the residual bacterial cells. After washing several times with distilled water, the cellulosic material was homogenized for 15 min with an Ultra-turrax® T25 Basic homogenizer (Ika-Werke, Stanfen, Germany) at 12,000 rpm and finally freeze-dried at −55°C and 0.63 mbar for 24 h using an ALPHA 1-2 LDplus freeze dryer (Martin Christ, Osterode am Harz, Germany).

2.4. Production of CNCs from the cellulose derived from agri-food wastes

The conversion of macro-sized cellulose to cellulose nanocrystals was performed by acid hydrolysis, using both sulfuric and hydrochloric acid. Specifically, 12 g of freeze-dried cellulose were added to 88 mL of distilled water. Then, 1 g of the stock dispersion was added to the acid solution (15 g of sulfuric acid – H_2SO_4, 58% v/v or hydrochloric acid – HCl 33% v/v). To promote the penetration of the acid inside the cellulosic network, cellulose-based aqueous dispersions were

TABLE 1 Composition of garlic stalk, corncob, and giant cane cut-up as reported in previous works.

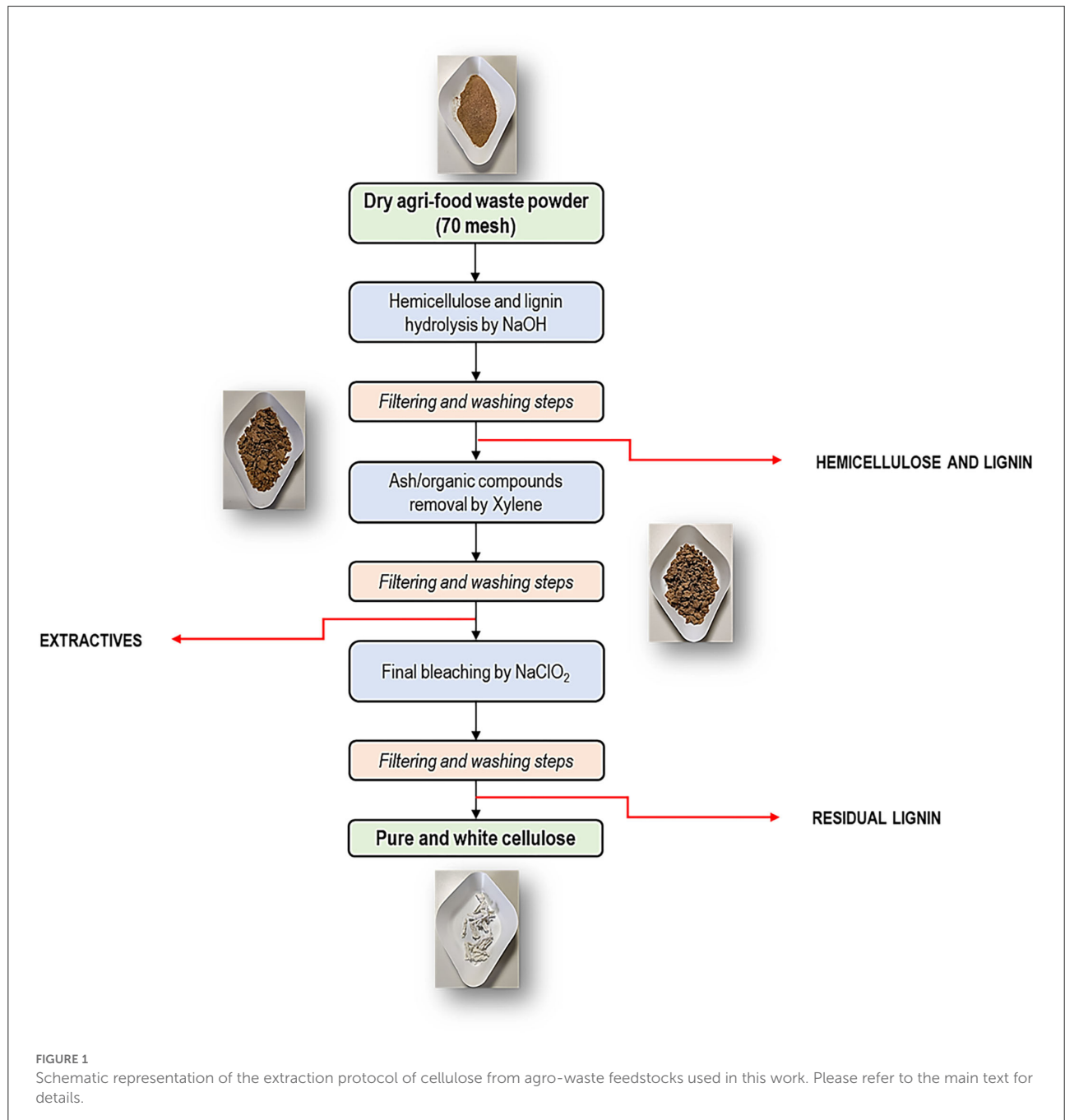| Substrate	Components				Reference
	Cellulose (%)	Hemicellulose (%)	Lignin (%)	Extracts and ash (%)	
Garlic stalk	49.80 ± 1.80	17.50 ± 0.90	28.60 ± 0.70	2.50 ± 0.10	Reddy and Rhim (2018)
Corncob	38.80 ± 2.50	41.40 ± 5.20	11.90 ± 2.30	2.88 ± 0.11	Pointner et al. (2016)
Giant cane cut-up	33.68 ± 3.93	24.62 ± 6.28	22.19 ± 2.73	14.20 ± 4.20	Corno et al. (2016)

FIGURE 1
Schematic representation of the extraction protocol of cellulose from agro-waste feedstocks used in this work. Please refer to the main text for details.

mixed by Ultra-turrax at 8,000 rpm for 5 min before hydrolysis. The hydrolytic process with sulfuric acid was performed under magnetic stirring (400 rpm) at $55 \pm 1°C$ for 120 min, while that involving hydrochloric acid was performed under gentle magnetic stirring at $60 \pm 1°C$ for 240 min. The hydrolysis reaction was terminated by adding 14 mL of cold distilled water, followed by centrifugation at 10,000 rpm for 15 min up to four times utilizing a Frontier^{TM} 5000 Series Multi centrifuge (Ohaus, Parsippany, USA). Between each centrifugation cycle, CNCs were collected at the bottom of the centrifuge tubes as pellets, while the acidic supernatant was discarded and replaced with fresh distilled water, followed by pellet redispersion at 3,000 rpm for 3 min. Finally, pH was adjusted to neutrality using a dialysis tube against deionized water, (MW cut off = 12,000) (Sigma-Aldrich, Milan, Italy). For comparison purposes, nanocrystals from bacterial cellulose (BCNCs) as a pure counterpart were also obtained using the same hydrolytic procedure as described for agro-waste feedstocks.

2.5. Analyses

For all the samples, the yield of both the cellulose extraction (Y_C, Equation 1) and hydrolysis (Y_{CNCs}, Equation 2) processes was determined gravimetrically with an HS43S-MC halogen-lamp moisture-content analyzer (Mettler Toledo, Greifensee, Switzerland) set at 105°C.

$$Y_C \ (\% \ DW_b) = \frac{m_{C.R., \ i}}{m_{0, \ i}} \qquad (1)$$

$$Y_{CNCs} \ (\% \ DW_{C.R.}) = \frac{m_{CNCs, \ i}}{m_{C.R., \ i}} \qquad (2)$$

In particular, $m_{C.R.,i}$ represents the mass of dry cellulosic residue extracted from the interest biomass (i = garlic stalk, corncob, and giant cane cut-up), $m_{0,i}$ stands for the initial amount of dry biomass undergoing the extraction process (2 g), and $m_{CNCs,i}$ is the dry mass of cellulose nanocrystals retrieved from the acid hydrolysis process of the i-th raw material.

Solid-state 13C Cross-Polarization Magic Angle Spinning (CP-MAS) spectra were collected at 125.76 MHz on an Avance 500 MHz NMR Spectrometer (Bruker Italia s.r.l., Milan, Italy), operating at a magnetic field of 11.7 T and equipped with a 4 mm MAS probe, spinning the sample at the magic angle up to 15 kHz, which, with the addition of high power 1H decoupling capability, allows the decrease or the elimination of homo and heteronuclear anisotropies. The chemical shifts were recorded relative to the glycine standard that was previously acquired (C=O signal: 176.03 ppm, relative to tetramethylsilane reference). All the samples were prepared by packing them in Zirconia (ZrO_2) rotors, closed with Kel-F caps (50 μL internal volume) and the MAS rate was optimized to 10 kHz, after having run some experiments in the range of 2–15 kHz. Cross-polarization (CP) spectra, under Hartmann–Hahn conditions,

were recorded with a variable spin-lock sequence (ramp CP-MAS) and a Contact time (CT) of 1 ms, optimized into a range between 1 and 5 ms. The following acquisition conditions were also applied: repetition time (d1) = 2 s, 1H 90° pulse length (p1) = 3.4 μs, spectral width (sw) = 240 ppm (30303.03 Hz) and acquisition Time (AQ) = 46 ms.

The crystallinity index (Cr.I.) related to the percentage of crystalline domains existing in the cellulose fibrils of different cellulose-based samples was calculated considering the region of the C4 13C CPMAS signals associated with the carbon C4 of the glucose units in the cellulose polymer chain, by comparing the area of C4 peak, in the range 86–92 ppm (crystalline domain), with that of the up-field C4 signal, in the range 80–86 ppm, related to the less ordered (amorphous) domains in the cellulose fibrils (Focher et al., 2001; Vismara et al., 2009). The software used for the comparison of interest areas was "MestReNova 14.1.2" (Mestrelab Research S.L., Santiago de Compostela, Spain), and the Global Spectral Deconvolution (GSD) analysis algorithm (Focher et al., 2001), able to apply an automatic multiplet deconvolution to the whole spectrum and fully characterize each fit peak (chemical shift, peak width, area, intensity, etc.) was launched. The Cr.I. (%) was finally calculated according to Equation (3), as follows:
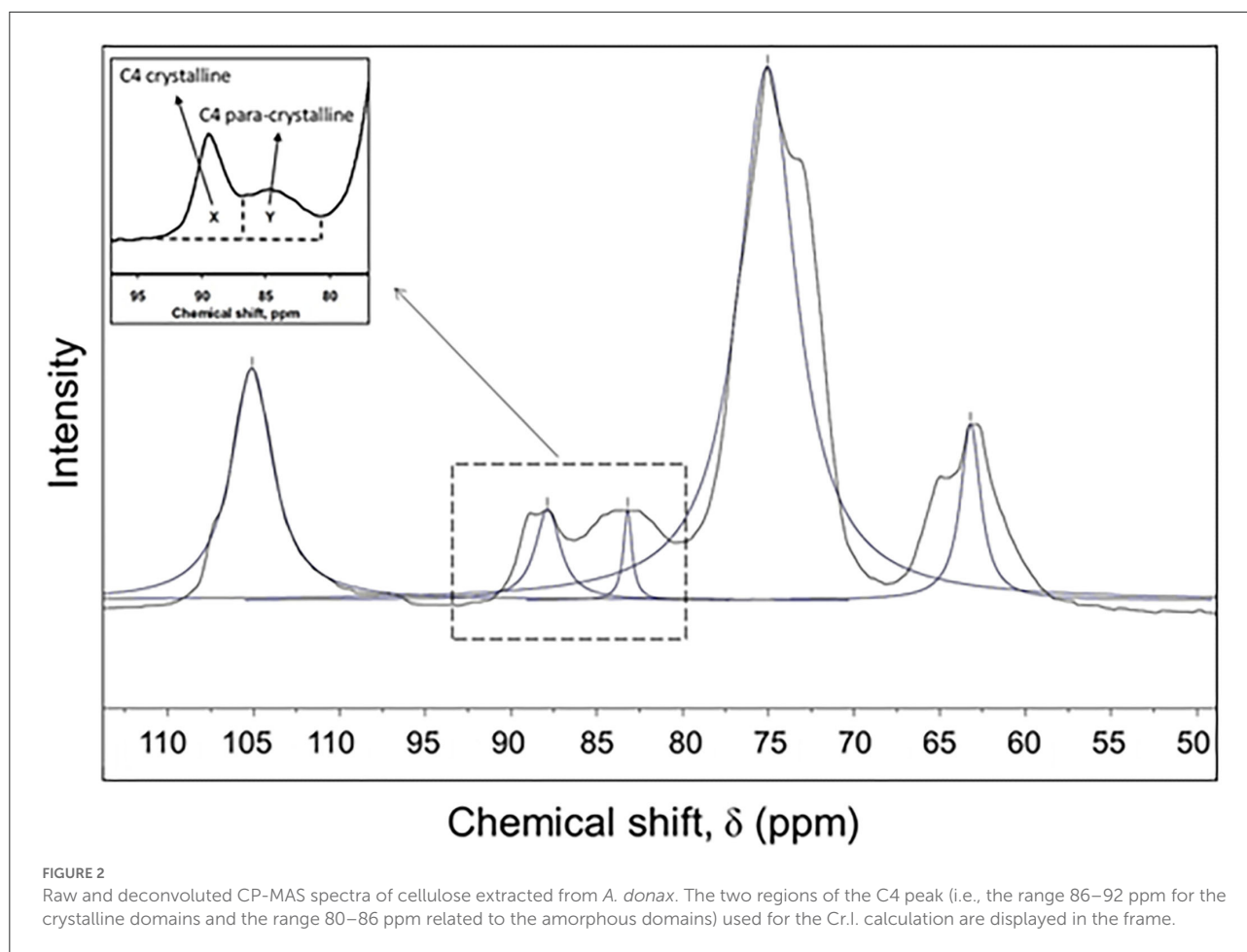
$$Cr.I. \ (\%) = \frac{x}{x + y} \cdot 100 \qquad (3)$$

Where x represents the C4 crystalline area below the interest peak, while y stands for the C4 para-crystalline one. For clarity purposes, the GSD-derived plot obtained from the NMR spectrum of the giant cane cut-up derived cellulose is reported in Figure 2, with the insert pointing to the regions (i.e., C4 crystalline and C4 para-crystalline) addressed for the Cr.I. calculation.

Solid-state Fourier Transform Infrared Spectroscopy (FT-IR) analysis was performed using a Spectrum 100 instrument (Perkin Elmer Inc., Waltham, MA), coupled with an Attenuated Total Reflectance (ATR) accessory and a Ge/Ge crystal, fixed at an incident angle of 45°. All spectra were collected at a resolution of 4 cm^{-1} over a wavenumber range between 4,000 cm^{-1} and 800 cm^{-1} and resulting from an average of 180 scans. A background scan of clean Ge crystal in air was acquired before each scan.

Basic information about the morphological features of cellulose was collected using a Nikon Eclipse ME600 Inspection optical microscope (Nikon Instruments, Sesto Fiorentino, Italy), equipped with a Nikon DS-Fi3 digital camera (Nikon Instruments, Sesto Fiorentino, Italy) using magnifications of 10×, 20×, and 50×. Microscopic images were captured by NIS-Element software (Nikon Instruments, Sesto Fiorentino, Italy).

In-depth morphological and size features of CNCs were determined using a Tosca^{TM} 400 AFM (Anton Paar Italia Srl, Rivoli, Italy) in contact resonance amplitude imaging (CRAI) mode. Toward this goal, an Arrow-FMR-10 Force

FIGURE 2
Raw and deconvoluted CP-MAS spectra of cellulose extracted from *A. donax*. The two regions of the C4 peak (i.e., the range 86−92 ppm for the crystalline domains and the range 80−86 ppm related to the amorphous domains) used for the Cr.I. calculation are displayed in the frame.

Modulation probe (Nanoworld, Neuchâtel, Switzerland) featuring a rectangular cantilever with a triangular free end and a tetrahedral tip with a typical height of 10–15 μm was used. Additionally, the tip radius of curvature is ∼10 nm. The cantilever has a spring constant and resonance frequency of 2.8 N m^{-1} and 75 kHz, respectively. For the analyses, approximately 100 μl of diluted CNC water dispersion (∼0.1 mg/mL) were dropped onto a mica disc substrate (Ted Pella Inc., Redding, California). Dimensional calculations and image editing were conducted *via* Tosca Analysis Software (version 7.30, Anton Paar, Graz, Austria). The mean values reported for each CNCs dimension were calculated over at least five images, from which at least ten measurements were taken.

The size distribution of CNCs was measured by photon correlation spectroscopy experiments using a dynamic light scattering (DLS) Nanotrac Flex *In-situ* Analyzer (MicroTrac GmbH, Krefeld, German). Tests were carried out at 25°C, with a stabilization time of 60 s, and using viscosity (0.8872 cP) and refractive index (1.33) of water as reference values. The software used the non-negative least squares algorithm to retrieve the size distribution.

The ζ-potential of CNCs aqueous solutions was investigated by electrophoretic light scattering (ELS) analysis, using a Litesizer^{TM} 500 (Anton Paar, Rivoli, Italy) system at neutral pH. For each sample, at least three replicates were performed.

Transmission electron microscopy (TEM) images of BCNCs were captured using a LEO 912 AB energy-filtering transmission electron microscope (EF-TEM, Carl Zeiss, Oberkochen, Germany) operating at 80 kV. Digital images were recorded with a ProScan 1K Slow-Scan CCD camera (Proscan, Scheuring, Germany). Samples for TEM analyses were prepared by drop-casting a few mL of a 0.2% wt. BCNCs dispersion onto Formvar-coated Cu grids (400-mesh) and letting the samples rest for 24 h at room temperature to allow water evaporation.

2.6. Statistical analysis

Data were analyzed using Statgraphics Plus 4.0 software (STSC, Rockville, MD, USA), and a one-way analysis of variance was used to check for differences among samples. The

significance level (p) was fixed at 0.05. Unless otherwise stated, all the analyses were performed in triplicate.

3. Results and discussion

3.1. Macro-sized cellulose extracted from biomass: Yield and physicochemical characterization

Cellulose was extracted from the pristine biomasses through a cascaded chemical procedure, as schematically depicted in Figure 1. Each step of the proposed protocol had the main goal of sequentially removing all the molecules other than cellulose (i.e., hemicellulose, lignin, ash, and organic compounds). In total, this procedure took approximately 6 h. The thermogravimetric measurements revealed that the ultimate process yields were as high as $35.73 \pm 0.95\%$ DW$_b$, $37.15 \pm 2.75\%$ DW$_b$, and $39.10 \pm 1.69\%$ DW$_b$ for garlic stalk, corncob, and giant cane cut-up samples, respectively (Table 2). These results clearly demonstrate the possibility of efficiently recovering cellulose from all the investigated matrices by a simple and fast chemical procedure, with ultimate yield values close to the theoretical ones (Table 1).

Information on the quality and chemical structure of cellulose extracted from garlic stalk, giant cane cut-up, and corncob was acquired by both FT-IR and 13C CP MAS NMR. FT-IR spectra are displayed in Figure 3. At first glance, it can be seen clearly that the individual patterns are very similar, suggesting an almost identical chemical composition of the biomass extracted from the three lignocellulosic wastes. More specifically, according to the assignments by Halib et al. (2012) and Atykyan et al. (2020), the characteristic absorption peaks of cellulose at ∼3,400 cm^{-1} and ∼2,900 cm^{-1} are attributed to the O-H and C-H stretching vibrations, respectively, while the absorption peak at 1,650 cm^{-1} was attributed to the O-H deformational vibration of the absorbed water. The peak assigned to the C-H and C-O vibrations of the polysaccharide ring of cellulose is centered between 1,300 and 1,400 cm^{-1}, whereas the peak at 1,460 cm^{-1} corresponds to CH$_2$ bending. The peaks associated with the vibration of C-O-C in the pyranose ring are centered at 1,178 and 1,060 cm^{-1} (Halib et al., 2012; Atykyan et al., 2020). The subtle peak at ∼900 cm^{-1} was attributed to the β-1,4 bond vibrations. Finally, it is interesting to note the peak at 1,670 cm^{-1}, which has been ascribed to the C=O stretching vibration of the carbonyl and acetyl groups of the xylan components of hemicellulose (Fiore et al., 2014). This observation seems to suggest a possible contamination of the main cellulosic residue (Fiore et al., 2014). For comparison purposes, the FT-IR spectra of BC and filter paper were reported in Figure 3. Also in this case, there is a clear correspondence of the different spectra obtained from the lignocellulosic biomass and the spectra of BC and commercial cellulose. The different shape of the peak centered at 3,350 cm^{-1} for the BC spectrum

(thinner than the bumpy band of plant cellulose) is thought to be due both to the higher crystallinity of BC compared to plant cellulose (Azeredo et al., 2019) and to the different crystalline structure between the triclinic I$_\alpha$ crystalline pattern of BC and the monoclinic I$_\beta$ pattern of plant cellulose. At the same time, this different shape has also been ascribed to a more ordered and pure structure of BC (Seoane et al., 2017). Therefore, from the comparison of the FTIR spectra reported in Figure 3, it can be inferred that the cellulose extracted form the agri-food waste has not the same degree of purity of BC, due to possible residues of other plant components such as hemicellulose and lignin.

More detailed information on the purity of the biomass obtained after the extraction procedure has been obtained through 13C CP MAS NMR. In full agreement with the findings of Park et al. (2009), Figure 4 highlights a full correspondence between the NMR spectra obtained from the agri-food biomass and the NMR reference spectrum of pure cellulose (BC). This correspondence was particularly clear in the correspondence between the C4 and C6 crystalline regions, C4 para-crystalline region, and C2,3,5 fractions (Focher et al., 2001), especially for corncob and giant cane cut-up samples. The presence of a subtle peak at 175.70 ppm for the garlic stalk-derived cellulose may indicate the presence of some organic compounds not yet completely removed after the purification step (Park et al., 2009).
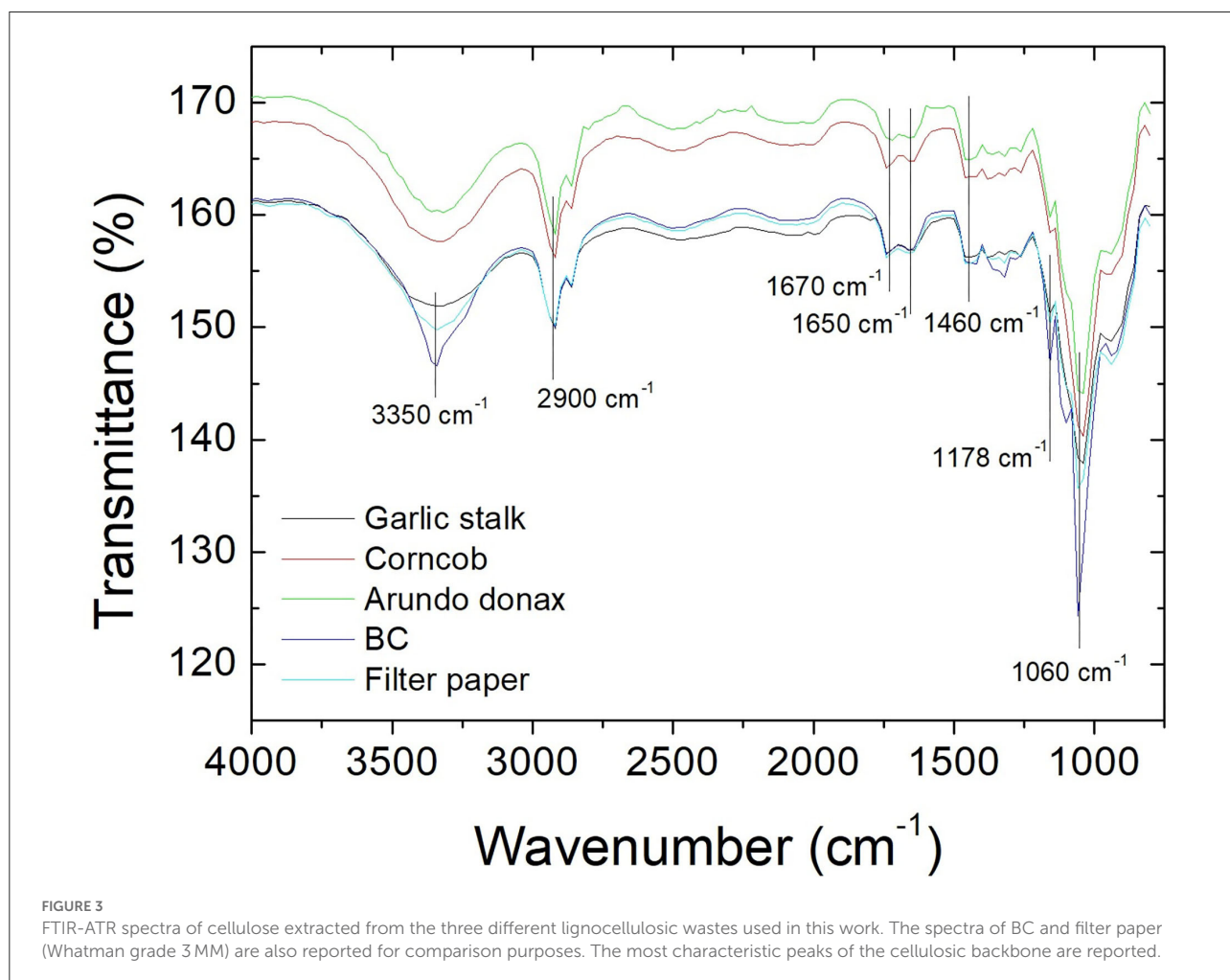
These results confirm that the biomass obtained after the extraction procedure was represented by high-purity cellulose, due to the absence of unpredictable signals coming from other fibrous components (e.g., hemicellulose, and lignin). This statement was supported by some evidence in the literature. Huang et al. (2017) observed that, in lignin samples, the characteristic peaks revealing the presence of such a molecule within NMR spectra stood within the aromatic region (160–103 ppm), and in the oxygenated and non-oxygenated regions (86–50 ppm). In a study by Zheng et al. (2015), different patterns with a single sharped peak in the region of 100–60 ppm were detected in hemicellulosic samples. All of the aforementioned regions were characterized by the presence of an up-field wing which might be attributed to the less ordered domains in the cellulose fibrils (Vismara et al., 2009).

13C CP MAS NMR spectra also allowed the calculation of the "crystallinity index" (Cr.I.) by means of Equation 3. As reported in Table 2, the agro-wastes-derived cellulose exhibited a larger number of crystalline domains over the amorphous ones. Specifically, Cr.I. average values were 73.84, 82.82, and 75.04% for garlic stalk, corncob, and giant cane cut-up, respectively (Table 2). These values were in line with those reported in the literature. For example, the Cr.I. of cotton linter-derived cellulose was ∼72.2% (Park et al., 2009), while Bahloul et al. (2021) calculated a Cr.I. of ∼62% after the extraction of cellulose from eggplant. By comparison, the crystallinity of bacterial cellulose (as a pure counterpart) was ∼70–80% (Vazquez et al., 2013) and 71.2% (Watanabe et al., 1998).

TABLE 2   Yield and Cr.I. of cellulose and yield and ζ-potential of CNCs extracted from garlic stalk, corncob, and giant cane cut-up.

Substrate	Cellulose		Cellulose Nanocrystals (CNCs)			
	Y_C (% DW_b)	Cr.I. (%)	Y_{CNCs} (% $DW_{C.R.}$)		ζ-potential	
			H_2SO_4	HCl	H_2SO_4	HCl
Garlic stalk	35.73 ± 0.95^a	73.84	$41.98 \pm 2.65^{a,A}$	$50.56 \pm 3.10^{a,B}$	$-27.17 \pm 0.31^{a,A}$	$-12.77 \pm 0.40^{a,B}$
Corn cob	37.15 ± 2.75^a	82.82	$40.87 \pm 3.15^{a,A}$	$49.73 \pm 1.45^{a,B}$	$-31.73 \pm 0.35^{b,A}$	$-13.77 \pm 0.51^{a,B}$
Giant cane cut-up	39.10 ± 1.69^a	75.04	$42.50 \pm 0.81^{a,A}$	$53.24 \pm 2.65^{a,B}$	$-32.93 \pm 0.25^{b,A}$	$-15.67 \pm 0.60^{b,B}$

Results are expressed as mean $\pm$ standard deviation. In the case of yield and ζ-potential associated to CNCs, different superscript lowercase and uppercase letters express significant differences among mean values as a function of substrate and hydrolyzing agent, respectively ($p < 0.05$).

FIGURE 3
FTIR-ATR spectra of cellulose extracted from the three different lignocellulosic wastes used in this work. The spectra of BC and filter paper (Whatman grade 3 MM) are also reported for comparison purposes. The most characteristic peaks of the cellulosic backbone are reported.

A preliminary morphological assessment of the cellulose extracted from garlic stalk, corncob, and giant cane cut-up was performed by optical microscopy analysis (Figure 5). Cellulose from all three lignocellulosic wastes was represented by a fibrous morphology, as confirmed by previous similar works (Luan et al., 2012; Vanderghem et al., 2012; Arantes et al., 2017; Wu and Cheng, 2017). Moreover, the overall length of the cellulose fibers was up to 1 mm, with a width varying from ~10 to ~15 µm.

3.2. Production of CNCs from agri-food wastes-derived cellulose *via* acid hydrolysis

Although low environmental impact approaches (e.g., enzymatic hydrolysis) have recently been proposed (Rovera et al., 2018, 2020), acid hydrolysis remains the most commonly used, efficient, and faster method to synthesize CNCs
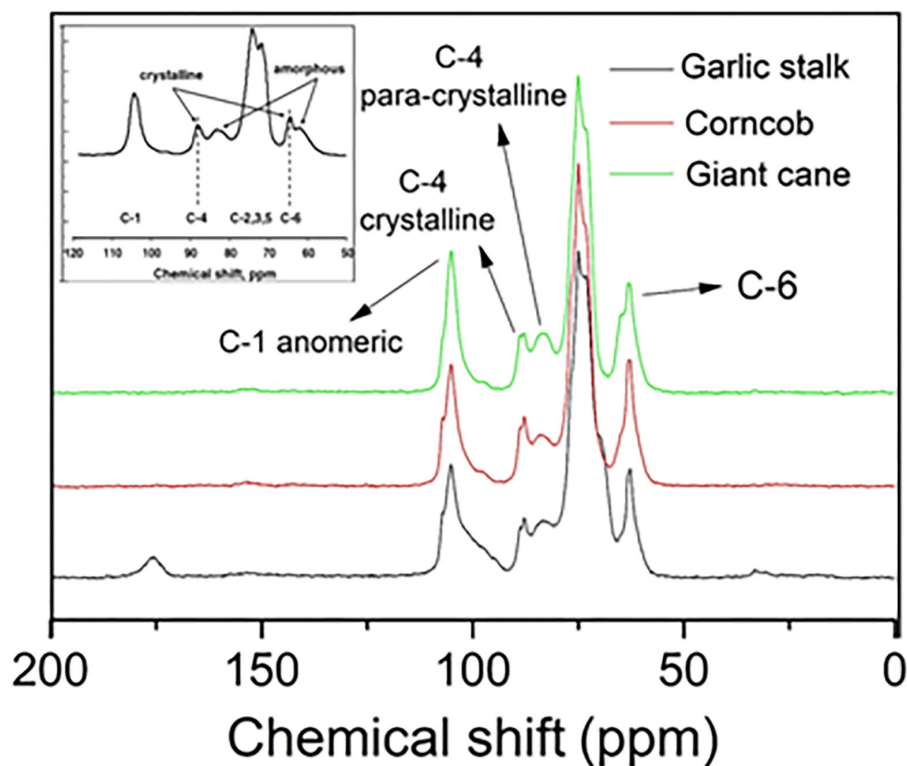
FIGURE 4
^{13}C CP MAS solid-state NMR spectra of garlic stalk, giant cane, and corncob-derived cellulose. The insert shows the spectrum of the pure bacterial counterpart, as retrieved from the work of Park et al. (2009).

(Habibi et al., 2010). In this work, the cellulosic substrate obtained from garlic stalk, corncob, and giant cane cut-up was subjected to acid hydrolysis to isolate the crystalline domains from the amorphous regions of the cellulosic backbone, eventually obtaining CNCs. By using a 58 % (v/v) sulfuric acid solution, the ultimate yield was as high as 41.98 ± 2.65 % DW$_{C.R.}$, 40.87 ± 3.15 % DW$_{C.R.}$, and 42.50 ± 0.81 % DW$_{C.R.}$ for CNCs derived from garlic stalk, corncob, and giant cane cut-up, respectively (Table 2). These results are in line with those found by Reddy and Rhim (2018), who reported a CNCs yield of ~39.5% from garlic skin utilizing 45% (v/v) of sulfuric acid for 2 h at 60°C. Silvério et al. (2013), working with cellulose extracted from corncob, reported a yield of 57 and 50% by using a 9.17 M of sulfuric acid solution at 45°C, for 30 and 60 min, respectively. The same authors obtained a 46% yield for CNCs generated *via* a 90 min contact with sulfuric acid. Instead, using a 33% (v/v) hydrochloric acid solution, the yield of hydrolysis was significantly higher for all the investigated substrates (50.56 ± 3.10 % DW$_{C.R.}$, 49.73 ± 1.45 % DW$_{C.R.}$, and 53.24 ± 2.65 % DW$_{C.R.}$ for CNCs derived from garlic stalk, corncob, and giant cane cut-up, respectively).

The stability of the CNCs water suspensions was evaluated by measuring the ζ-potential by DLS analysis. For the CNC derived from all the three agro-wastes, a mean value of ζ > −30 mV was measured when sulfuric acid was used, whereas ζ < −15 mV was obtained as an average for CNCs derived from hydrochloric acid. According to a study by Clogston and Patri (2011), ζ-potential values of > |30| mV are deemed the minimum requirement to produce a stable colloidal dispersion. The greater stability of the CNCs suspension obtained using sulfuric acid can be explained by the esterification of the hydroxyl groups on the C6 of the cellulosic backbone to form sulfate groups (i.e., –SO$_4^{-2}$), hence negative charges that were responsible for intermolecular repulsion forces. In contrast, ζ-potential values <|30| mV pertain to less stable colloidal dispersions, which most likely will undergo aggregation, flocculation, and phase separation over time. In this specific case, the absence of a net charge on the CNCs surface will bring to flocculation due to the tendency of CNCs to aggregate by H-bonding.

A morphological investigation of CNCs was first performed by AFM (Figure 6). Figures 6a–d, in particular, shows the AFM images of CNCs obtained after acid hydrolysis of garlic stalk (a and b), corncob (c), and giant cane cut-up (d) extracted by means of sulfuric acid. Nanocrystals generated from a sulfuric
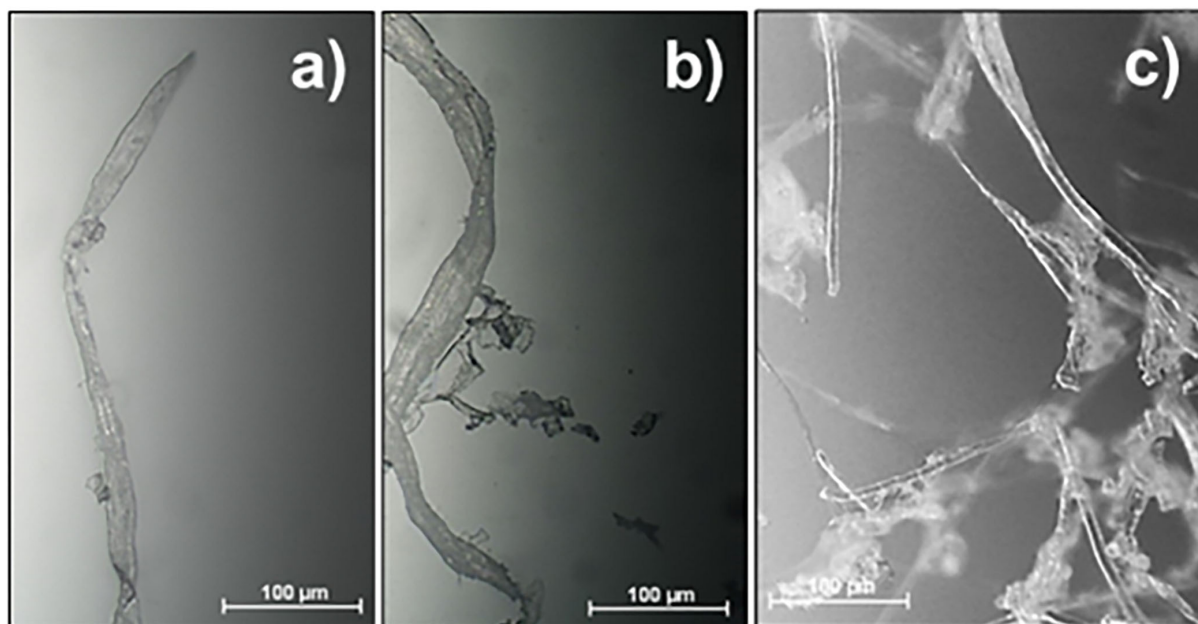
FIGURE 5
Optical microscope images of corncob **(a)**, giant cane cut-up **(b)**, and garlic stalk **(c)**, at 10× magnification.

acid-driven hydrolysis process showed a typical needle-like shape, with an apparent averaged size (length) according to the following order: garlic stalks>corncob>giant cane. CNCs from giant cane cut-up extracted using hydrochloric acid (Figures 6e, f) showed a less defined shape, with a frayed morphology and a generally larger size (300–450 nm) than CNCs obtained using sulfuric acid. Similar results were observed in the case of garlic stalk and corncob.

The different sizes of CNCs treated with the two acids were confirmed by the particle size distribution measurements (Figure 7). Although DLS is not the most suitable analytical technique to determine the absolute size distribution of non-spherical particles (Rovera et al., 2018), it has been demonstrated that it is useful to monitor the relative difference in the size of particles obtained according to different treatments/setups. Figure 7A shows the bimodal size distribution of the nano-sized CNCs generated from sulfuric acid-treated cellulose. The position and intensity of the two main peaks were matrix-dependent. In particular, in CNCs derived from giant cane cut-up and corncob agro-wastes, the most intense peak was centered at ∼90 and 120 nm, respectively, while the less intense one was centered at around 450 nm for both types of CNCs. Similarly, the size distribution of CNCs from garlic stalks showed a more intense peak at ∼190 nm, while a less intense peak was observed at 750 nm. When the hydrolysis was carried out using hydrochloric acid, a general shift toward larger sizes was observed for the CNCs, though with an identical bimodal distribution (Figure 7B). More specifically, in CNCs derived from corncob and giant cane cut-up agro-wastes, the largest peak in intensity was centered at ∼900–1,200 nm, while the less intense one was centered at ∼260 nm. CNCs from garlic stalks exhibited the largest peak in intensity centered at ∼1.8 μm, while a less intense peak was centered at ∼630 nm (Figure 7B). These results thus seem to confirm our previous observations with AFM (Figure 6).

Based on the findings arising from both AFM and DLS analyses, it can be said that the hydrolytic process of cellulose from three different wastes provided non-homogeneous size distributions of the CNCs population, that is, two main size domains were detected when both sulfuric and hydrochloric acid were used. However, it seemed that the process mediated by sulfuric acid was more efficient in providing CNCs with smaller sizes. Our findings are in line with those reported in previous works. Silvério et al. (2013) reported a size distribution centered at ∼290 and ∼195 nm for CNCs extracted by acid hydrolysis (sulfuric acid 9.17 M) at 45°C, for 30 or 90 min. Similarly, Barana et al. (2016) reported an overall length of CNCs from *Arundo donax* of ∼200 nm (60% H_2SO_4 at 55°C for 1 or 2 h). Kallel et al. (2016) found an average length of ∼480 nm for CNCs extracted from garlic stalks by using a 65% (v/v) H_2SO_4 solution (45°C for 40 min).
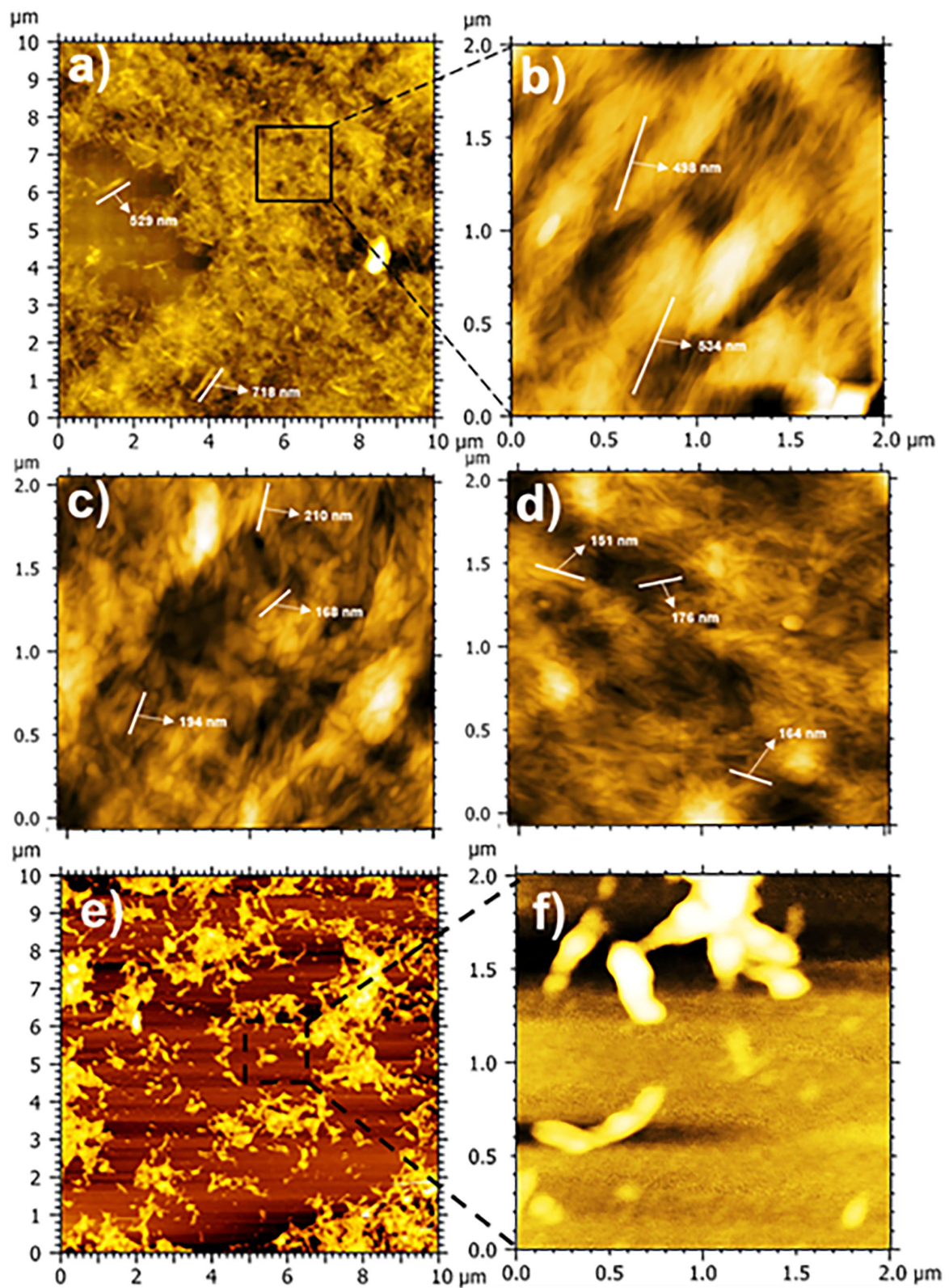
FIGURE 6
Atomic Force Microscopy (AFM) images of CNCs derived from garlic stalk **(a, b)**, corncob **(c)**, and giant cane cut-up **(d)** extracted by means of sulfuric acid. Panels **(e, f)** show AFM images of CNCs from giant cane cut-up extracted using hydrochloric acid.
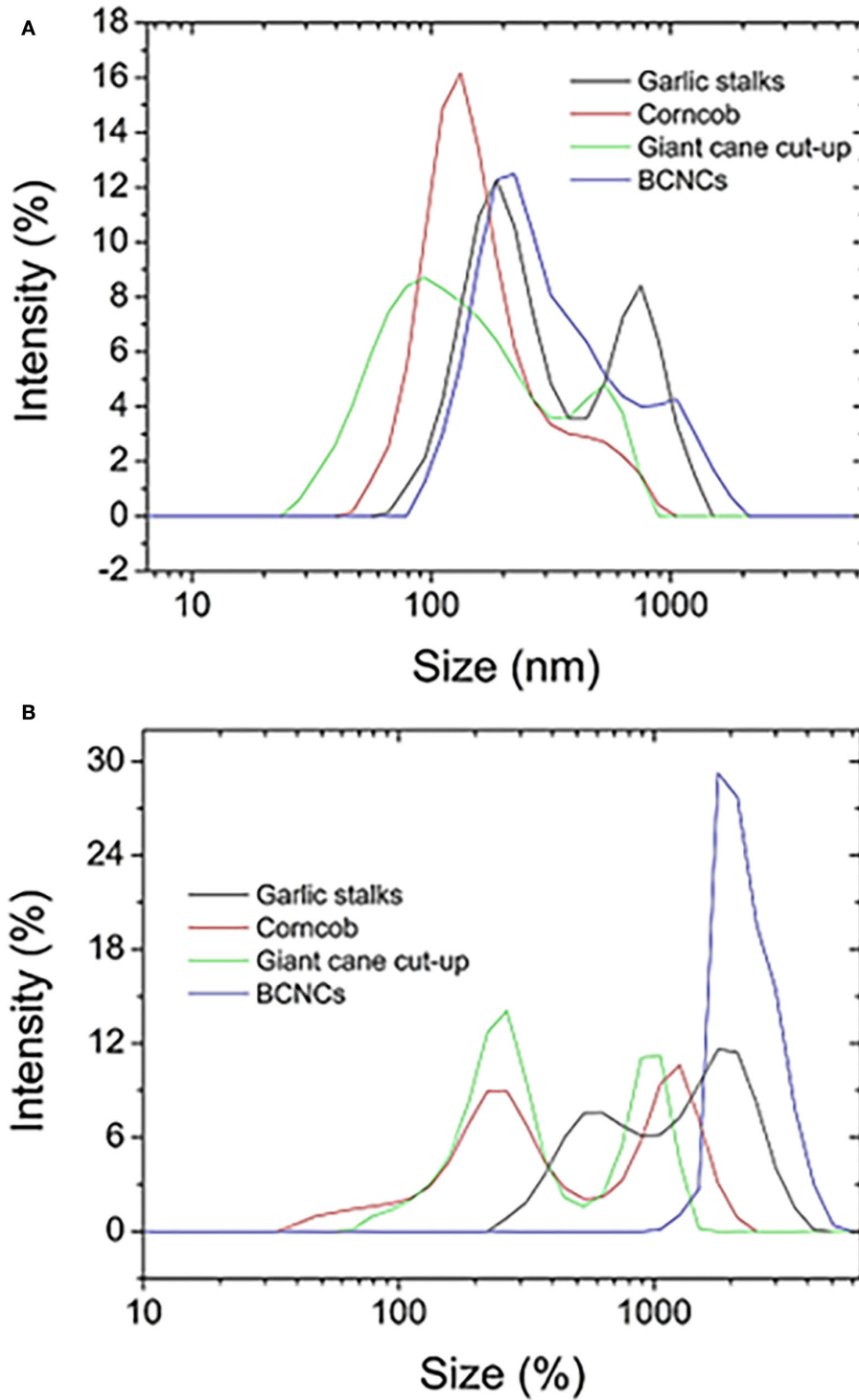
FIGURE 7
Size distribution by DLS analysis of CNCs derived from garlic stalk, corncob, and giant cane cut-up biomasses after acid hydrolysis by sulfuric **(A)** and hydrochloric **(B)** acid. For comparison purposes, the size distribution of CNCs from acid hydrolysis of cellulose produced by *K. sucrofermentans* has also been reported.

## 3.3. Comparison between CNCs from agri-food wastes and BCNCs

With the goal of gathering further information on the quality of CNCs extracted from lignocellulosic wastes, a comparison with CNCs extracted from bacterial cellulose (BC) was performed, in consideration of the fact that BC is inherently devoid of contaminating molecules, such as lignin, pectins, hemicelluloses, etc., typical of cellulose of plant origin; that is, BC has a high purity degree (Gorgieva and Trček, 2019).

Acid hydrolysis of BC yielded $51.61 \pm 1.51\%$ and $69.83 \pm 3.94\%$ when sulfuric acid and hydrochloric acid were used, respectively. This means that, compared with the extraction of CNCs from cellulose from agri-food wastes, a $+ 23.3\%$ in the final yield was obtained for the sulfuric acid-mediated hydrolysis, whereas an average 1.4-fold increase was achieved with hydrochloric acid. The yield increase in the case of BC can be ascribed to the different ratios between amorphous and crystalline domains. In particular, the degree of crystallinity of BC is higher than that of plant-based cellulose (85–90% for bacterial cellulose vs. 65–75% for plant-based cellulose) (Sacui et al., 2014).

Additional morphological and dimensional information on BCNCs was obtained by TEM, AFM, and DLS analyses. BCNCs with a needle-like shape were obtained when both HCl (Figures 8a, c) and H_2SO_4 (Figure 8b) were used, in contrast to what was observed for CNCs obtained from the lignocellulosic wastes (in this case, HCl hydrolysis yielded irregularly shaped nanocrystals, see Figures 6c, d). Apparently, BCNCs were wider than the plant-derived counterpart, thus displaying average length and width of 390 ± 35 and 18 ± 3 nm, respectively. The DLS analysis confirmed a bimodal size distribution for BCNCs obtained *via* sulfuric acid, in agreement with Rollini et al. (2020), who found two main dimensional families ($\sim$240 nm and $\sim$1 μm) of BCNCs obtained using a 65% (v/v) sulfuric acid solution at $55 \pm 1°C$ for 2 h. Conversely, only one main peak centered at $\sim$2 μm was detected for BCNCs obtained using HCl. Irrespective of the acid used, a shift toward higher dimensions was observed for BCNCs, confirming what has been seen through TEM and AFM (Figure 8). Finally, the DLS pattern for BCNCs obtained using HCl (i.e., one main narrow peak) is typical of monodisperse systems, hence suggesting a better efficiency for HCl-mediated hydrolysis of BC over H_2SO_4 hydrolysis. Instead, Arserim-Uçar et al. (2021) detected a size distribution of BCNCs from 920 nm to $\sim$1 μm when a 4 N HCl (reagent grade 37% v/v) acid solution at 95 °C and 105 °C for 240 min was adopted.

4. Conclusions

In the present work, an easy and fast chemical procedure to extract cellulose from three different agri-food wastes (e.g., garlic stalk, corncob, and giant cane cut-up) was presented. Overall,
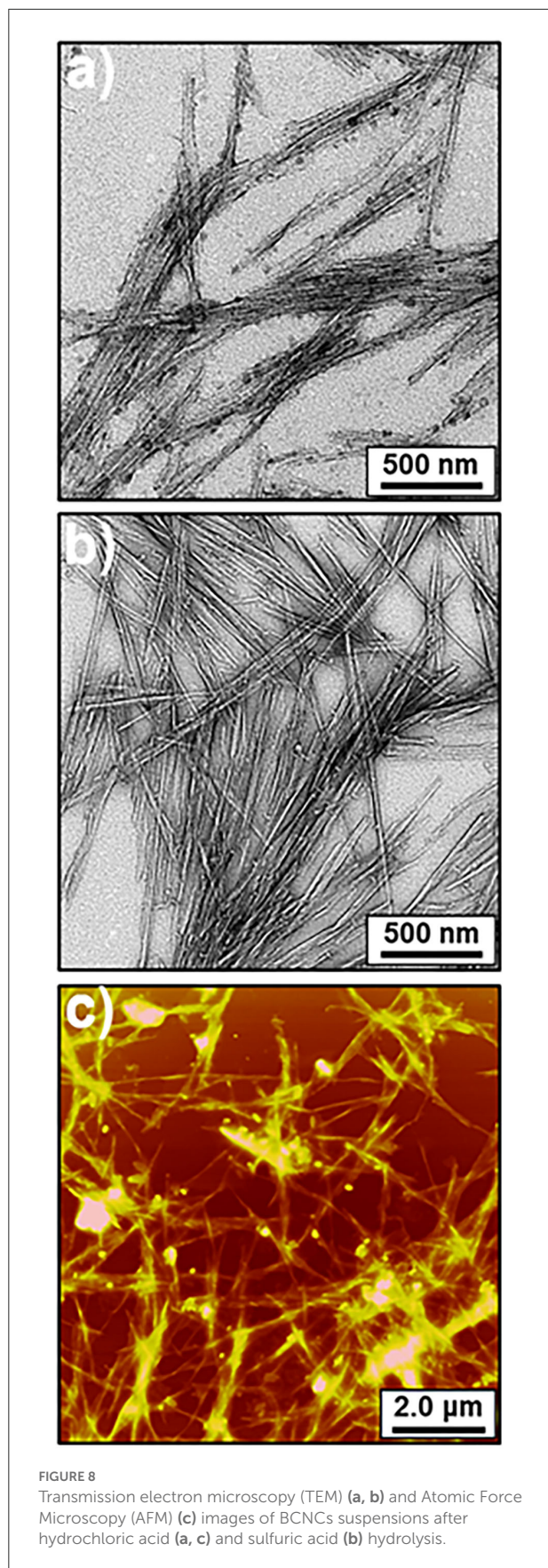
the approach used allowed the achievement of remarkable yields (>35%) of extraordinary high-quality grade cellulose, as demonstrated by spectroscopic analyses. The possibility of obtaining CNCs by acid hydrolysis was also demonstrated, whereby sulfuric acid seemed to provide CNCs with better morphological features than CNCs obtained with hydrochloric acid. The comparison with BCNCs revealed that the overall process was more efficient for BCs than for CNCs from lignocellulosic wastes in terms of yield and morphological quality of final nanocrystals, probably due to the higher crystallinity and purity of the original raw material. However, the proposed approach represents a feasible strategy for the valorization of wastes and/or residues of the agri-food sector to eventually obtain added-value products (macro-sized cellulose and CNCs) with potential applications in different fields, e.g., new materials for food packaging. Additional studies will focus on elucidating the role and interaction between the proposed cascade purification route and the processed biomass, with the purpose of developing a technological platform to give value to disparate cellulose sources, thus increasing the availability of high-added molecules to feed multiple industrial sectors.

Data availability statement

The raw data supporting the conclusions of this article will be made available by the authors, without undue reservation.

Author contributions

CR: conceptualization, data curation, investigation, methodology, and writing-original draft. DC: formal analysis, visualization, and writing-review and editing. TB: formal analysis. DB and MG: writing-review and editing. EC: investigation and methodology. SF: conceptualization, data curation, investigation, methodology, project administration, resources, supervision, visualization, validation, and writing-review and editing. All authors contributed to the article and approved the submitted version.

Conflict of interest

The authors declare that the research was conducted in the absence of any commercial or financial relationships that could be construed as a potential conflict of interest.

Publisher's note

All claims expressed in this article are solely those of the authors and do not necessarily represent those of their affiliated organizations, or those of the publisher, the editors and the reviewers. Any product that may be evaluated in this article, or claim that may be made by its manufacturer, is not guaranteed or endorsed by the publisher.

References

Abdul Khalil, H. P. S., Adnan, A. S., Yahya, E. B., Olaiya, N. G., Safrida, S., Hossain, M. S., et al. (2020). A review on plant cellulose nanofibre-based aerogels for biomedical applications. *Polymers* 12, 1759. doi: 10.3390/polym12081759

Arantes, A. C. C., Almeida, C. D. G., Dauzacker, L. C. L., Bianchi, M. L., Wood, D. F., Williams, T. G., et al. (2017). Renewable hybrid nanocatalyst from magnetite and cellulose for treatment of textile effluents. *Carbohydr. Polym.* 1, 101–107. doi: 10.1016/j.carbpol.2017.01.007

Arserim-Uçar, D. K., Korel, F., Liu, L., and Yam, K. L. (2021). Characterization of bacterial cellulose nanocrystals: effect of acid treatments and neutralization. *Food Chem.* 336, 127597. doi: 10.1016/j.foodchem.2020.127597

Atykyan, N., Revin, V., and Shutova, V. (2020). Raman and FT-IR Spectroscopy investigation the cellulose structural differences from bacteria Gluconacetobacter sucrofermentans during the different regimes of cultivation on a molasses media. *AMB Expr.* 10, 1–11. doi: 10.1186/s13568-020-01020-8

Azeredo, H. M. C., Barud, H., Farinas, C. S., Vasconcellos, V. M., and Claro, A. M. (2019). Bacterial cellulose as a raw material for food and food packaging applications. *Front. Sustain. Food Syst.* 3, 71–14. doi: 10.3389/fsufs.2019.00007

Bahloul, A., Kassab, Z., El Bouchti, M., Hannache, H., Oumam, M., El Achaby, M., et al. (2021). Micro-and nano-structures of cellulose from eggplant plant (*Solanum melongena L*) agricultural residue. *Carbohydr. Polym.* 253, 117311. doi: 10.1016/j.carbpol.2020.117311

Barana, D., Salanti, A., Orlandi, M., Ali, D. S., and Zoia, L. (2016). Biorefinery process for the simultaneous recovery of lignin, hemicelluloses, cellulose nanocrystals and silica from rice husk and Arundo donax. *Ind. Crops Prod.* 86, 31–39. doi: 10.1016/j.indcrop.2016.03.029

Calvo, M. V., Colombo, B., Corno, L., Eisele, G., Cosentino, C., Papa, G., et al. (2018). Bioconversion of giant cane for integrated production of biohydrogen, carboxylic acids, and polyhydroxyalkanoates (PHAs) in a

multistage biorefinery approach. *ACS Sust. Chem. Eng.* 6, 15361–15373. doi: 10.1021/acssuschemeng.8b03794

Ceotto, E., and Di Candilo. (2010). Shoot cuttings propagation of giant reed (*Arundo donax L.*) in water and moist soil: the path forward? *Biomass Bioen.* 34, 1614–1623. doi: 10.1016/j.biombioe.2010.06.002

Chen, D., Lawton, D., Thompson, M. R., and Liu, Q. (2012). Biocomposites reinforced with cellulose nanocrystals derived from potato peel waste. *Carbohydr. Polym.* 90, 709–716. doi: 10.1016/j.carbpol.2012.06.002

Chen, M., Xia, L., and Xue, P. (2007). Enzymatic hydrolysis of corncob and ethanol production from cellulosic hydrolysate. *Int. Biodeterior. Biodegradation.* 59, 85–89. doi: 10.1016/j.ibiod.2006.07.011

Cherubini, F., and Jungmeier, G. (2010). LCA of a biorefinery concept producing bioethanol, bioenergy, and chemicals from switchgrass. *Int. J. Life Cycle Assess.* 15, 53.–66. doi: 10.1007/s11367-009-0124-2

Clogston, J. D., and Patri, A. K. (2011). Zeta Potential Measurement. In: McNeil S. (eds) *Characterization of Nanoparticles Intended for Drug Delivery. Methods in Molecular Biology* (Methods and Protocols), vol 697. Humana Press. doi: 10.1007/978-1-60327-198-1_6

Corno, L., Lonati, S., Riva, C., Pilu, R., and Adani, F. (2016). Giant cane (*Arundo Donax L.*) can substitute traditional energy crops in producing energy by anaerobic digestion, reducing surface area and costs: a full-scale approach. *Bioresour. Technol.* 218, 826–832. doi: 10.1016/j.biortech.2016.07.050

Corno, L., Pilu, R., and Adani, F. (2014). Arundo donax L.: a non-food crop for bioenergy and bio-compound production. *Biotechnol. Adv.* 32, 1535–1549. doi: 10.1016/j.biotechadv.2014.10.006

FAOSTAT, 2016. Crops and livestock products. Available online at: https://www.fao.org/faostat/en/#data/QC (accessed 9 March 2022).

Fiore, V., Scalici, T., and Valenza, A. J. C. P. (2014). Characterization of a new natural fiber from *Arundo donax L.* as potential reinforcement of polymer composites. *Carbohydr. Polym.* 106, 77–83. doi: 10.1016/j.carbpol.2014.02.016

Focher, B., Palma, M. T., Canetti, M., Torri, G., Cosentino, C., Gastaldi, G., et al. (2001). Structural differences between non-wood plant celluloses: evidence from solid state NMR, vibrational spectroscopy and X-ray diffractometry. *Ind. Crops Prod.* 13, 193–208. doi: 10.1016/S0926-6690(00)00077-7

Ganguly, P., Sengupta, S., Das, P., and Bhowal, A. (2020). Valorization of food waste: extraction of cellulose, lignin and their application in energy use and water treatment. *Fuel* 280, 118581. doi: 10.1016/j.fuel.2020.118581

Gorgieva, S., and Trček, J. (2019). Bacterial cellulose: production, modification and perspectives in biomedical applications. *Nanomaterials* 9, 1352. doi: 10.3390/nano9101352

Habibi, Y., Lucia, L. A., and Rojas, O. J. (2010). Cellulose nanocrystals: chemistry, self-assembly, and applications. *Chem. Rev.* 110, 3479–3500. doi: 10.1021/cr900339w

Hafemann, E., Battisti, R., Marangoni, C., and Machado, R. A. (2019). Valorization of royal palm tree agroindustrial waste by isolating cellulose nanocrystals. *Carbohydr. Polym.* 218, 188–198. doi: 10.1016/j.carbpol.2019.04.086

Halib, N., Amin, M. C. I. M., and Ahmad, I. (2012). Physicochemical properties and characterization of nata de coco from local food industries as a source of cellulose. *Sains Malays.* 41, 205–211.

Huang, C., He, J., Narron, R., Wang, Y., and Yong, Q. (2017). Characterization of kraft lignin fractions obtained by sequential ultrafiltration and their potential application as a biobased component in blends with polyethylene. *ACS Sustain. Chem. Eng.* 5, 11770–11779. doi: 10.1021/acssuschemeng.7b03415

Ioannidou, O., Zabaniotou, A., Antonakou, E. V., Papazisi, K. M., Lappas, A. A., Athanassiou, C., et al. (2009). Investigating the potential for energy, fuel, materials and chemicals production from corn residues (cobs and stalks) by non-catalytic and catalytic pyrolysis in two reactor configurations. *Renew. Sust. Energ. Rev.* 13, 750–762. doi: 10.1016/j.rser.2008.01.004

Jayaramudu, J., Reddy, G., Varaprasad, K., Sadiku, E. R., Sinha-Ray, S., Varada Rajulu, A., et al. (2013). Preparation and properties of biodegradable films from Sterculia urens short fiber/cellulose green composites. *Carbohydr. Polym.* 93, 622–627. doi: 10.1016/j.carbpol.2013.01.032

Kallel, F., Bettaieb, F., Khiari, R., García, A., Bras, J., Chaabouni, S. E., et al. (2016). Isolation and structural characterization of cellulose nanocrystals extracted from garlic straw residues. *Ind. Crops Prod.* 87, 287–296. doi: 10.1016/j.indcrop.2016.04.060

Kallel, F., and Ellouz Chaabouni, S. (2017). Perspective of garlic processing wastes as low-cost substrates for production of high-added value products: a review. *Environ. Prog. Sustainable Energy* 36, 1765.–1777. doi: 10.1002/ep.12649

Lau, T., Harbourne, N., and Oruna-Concha, M. J. (2019). Valorisation of sweet corn (Zea mays) cob by extraction of valuable compounds. *Int. J. Food Sci.* 54, 1240–1246. doi: 10.1111/ijfs.14092

Liguoria, R., and Faraco, V. (2016). Biological processes for advancing lignocellulosic waste biorefinery by advocating circular economy. *Bioresour. Technol.* 215, 13–20. doi: 10.1016/j.biortech.2016.04.054

Luan, J., Wu, J., Zheng, Y., Song, W., Wang, G., Guo, J., et al. (2012). Impregnation of silver sulfadiazine into bacterial cellulose for antimicrobial and biocompatible wound dressing. *Biomed. Mater.* 7, 065006. doi: 10.1088/1748-6041/7/6/065006

McKendry, P. (2002). Energy production from biomass (Part 1): overview of biomass. *Bioresour. Technol.* 83, 37–46. doi: 10.1016/S0960-8524(01)00118-3

Méndez-Hernández, J. E., Loera, O., Méndez-Hernández, E. M., Herrera, E., Arce-Cervantes, O., Soto-Cruz, N. Ó., et al. (2019). Fungal pretreatment of corn stover by fomes sp. EUM1: simultaneous production of readily hydrolysable biomass and useful biocatalysts. *Waste Biomass Valori.* 10, 2637–2650. doi: 10.1007/s12649-018-0290-1

Mondal, M. I. H., and Haque, M.M.U. (2007). Effect of grafting methacrylate monomers onto jute constituents with a potassium per sulfate initiator catalyzed by Fe (II). *J. Appl. Polym. Sci.* 103, 2369–2375. doi: 10.1002/app.25276

Mondal, M. I. H., Yeasmin, M. S., and Rahman, M. S. (2015). Preparation of food grade carboxymethyl cellulose from corn husk agrowaste. *Int. J. Biol. Macromol.* 79, 144–150. doi: 10.1016/j.ijbiomac.2015.04.061

Moreno, L. M., Gorinstein, S., Medina, O. J., Palacios, J., and Muñoz, E. J. (2019). Valorization of garlic crops residues as precursors of cellulosic materials. *Waste Biomass Valori.* 11, 4767–4779. doi: 10.1007/s12649-019-00799-3

Mullen, C. A., Boateng, A. A., Goldberg, N. M., Lima, I. M., Laird, D. A., Hicks, K. B., et al. (2010). Bio-oil and bio-char production from corncobs and stover by fast pyrolysis. *Biomass Bioenergy* 34, 67–74. doi: 10.1016/j.biombioe.2009.09.012

Park, S., Johnson, D. K., Ishizawa, C. I., Parilla, P. A., and Davis, M. F. (2009). Measuring the crystallinity index of cellulose by solid state 13C nuclear magnetic resonance. *Cellulose* 16, 641–647. doi: 10.1007/s10570-009-9321-1

Peguero, D. A., Gold, M., Vandeweyer, D., Zurbrügg, C., and Mathis, A. (2022). A review of pretreatment methods to improve agri-food waste bioconversion by black soldier fly Larvae. *Front. Sustain. Food Syst.* 5, 745894. doi: 10.3389/fsufs.2021.745894

Pointner, M., Kuttner, P., Obrlik, T., Jager, A., and Kahr, H. (2016). "Composition of corncobs as a substrate for fermentation of biofuels," in *Proceeding of the Conference: Biosystems Engineering 2016, Vol.12* (Tartu, EST).

Rahman, M. M., and Netraval, A. N. (2016). Micro-fibrillated cellulose reinforced eco-friendly polymeric resin from non-edible 'Jatropha curcas' seed waste after biodiesel production. *RSC Adv.* 6, 47101–47111. doi: 10.1039/C6RA07749H

Reddy, J. P., and Rhim, J. W. (2018). Extraction and characterization of cellulose microfibers from agricultural wastes of onion and garlic. *J. Nat. Fibers.* 15, 465–473. doi: 10.1080/15440478.2014.945227

Reddy, N., and Yang, Y. (2005). Properties and potential applications of natural cellulose fibers from cornhusks. *Green Chem.* 7, 190–195. doi: 10.1039/b415102j

Rollini, M., Musatti, A., Cavicchioli, D., Bussini, D., Farris, S., Rovera, C., et al. (2020). From cheese whey permeate to Sakacin-A/bacterial cellulose nanocrystal conjugates for antimicrobial food packaging applications: a circular economy case study. *Sci. Rep.* 10, 21358. doi: 10.1038/s41598-020-78430-y

Rovera, C., Fiori, F., Trabattoni, S., Romano, D., and Farris, S. (2020). Enzymatic hydrolysis of bacterial cellulose for the production of nanocrystals for the food packaging industry. *Nanomaterials* 10, 735. doi: 10.3390/nano10040735

Rovera, C., Ghaani, M., Santo, N., Trabattoni, S., Olsson, R. T., Romano, D., et al. (2018). Enzymatic hydrolysis in the green production of bacterial cellulose nanocrystals. *ACS Sustainable Chem. Eng.* 6, 7725.–7734. doi: 10.1021/acssuschemeng.8b00600

Sacui, I. A., Nieuwendaal, R. C., Burnett, D. J., Stranick, S. J., Jorfi, M., Weder, C., et al. (2014). Comparison of the properties of cellulose nanocrystals and cellulose nanofibrils isolated from bacteria, tunicate, and wood processed using acid, enzymatic, mechanical, and oxidative methods. *ACS Appl. Mater. Interfaces* 6, 6127.–6138. doi: 10.1021/am500359f

Seoane, I. T., Cerrutti, P., Vasquez, A., Manfredi, L. B., and Cyras, V. P. (2017). Polyhydroxybutyrate-based nanocomposites with cellulose nanocrystals and bacterial cellulose. *J. Polym. Environ.* 25, 586.–598. doi: 10.1007/s10924-016-0838-8

Shiferaw, B., Prasanna, B. M., Hellin, J., and Banziger, M. (2011). Crops that feed the world 6. Past successes and future challenges to the role played by maize in global food security. *Food Secur.* 3, 307–327. doi: 10.1007/s12571-011-0140-5

Silvério, H. A., Neto, W. P. F., Dantas, N. O., and Pasquini, D. (2013). Extraction and characterization of cellulose nanocrystals from corncob for application as reinforcing agent in nanocomposites. *Ind. Crops. Prod*. 44, 427–436. doi: 10.1016/j.indcrop.2012.10.014

Sims, R. (2003). *Biomass and Resources Bioenergy Options for a Cleaner Environment in Developed and Developing Countries.* London, UK: Elsevier Science. doi: 10.1016/B978-008044351-5/50003-9

Sjöström, E. (1993). *Wood Chemistry: Fundamentals and Applications*. San Diego, USA: Academic Press.

Thomsen, M. H. (2005). Complex media from processing of agricultural crops for microbial fermentation. *Appl. Microbiol. Biotechnol*. 68, 598–606. doi: 10.1007/s00253-005-0056-0

Torre, P., Aliakbarian, B., Rivas, B. Dominguez, J.M., and Converti, A. (2008). Release of ferulic acid from corncobs by alkaline hydrolysis. *Biochem. Eng. J*. 40, 500–506. doi: 10.1016/j.bej.2008.02.005

USDA-NASS (2016). Agricultural statistics database. *National statistics for corn.* Available online at: https://www.nass.usda.gov/Statistics_by_Subject/index.php?sector=CROPS (accessed 29 September 2022).

Vanderghem, C., Jacquet, N., Danthine, S., Blecker, C., and Paquot, M. (2012). Effect of physicochemical characteristics of cellulosic substrates on enzymatic hydrolysis by means of a multi-stage process for cellobiose production. *Appl. Biochem. Biotechnol*. 166, 1423–1432. doi: 10.1007/s12010-011-9535-1

Vazquez, A., Foresti, M. L., Cerrutti, P., and Galvagno, M. (2013). Bacterial cellulose from simple and low cost production media by gluconacetobacter xylinus. *J. Polym. Environ*. 21, 545–554. doi: 10.1007/s10924-012-0541-3

Vismara, E., Melone, L., Gastaldi, G., Cosentino, C., and Torri, G. (2009). Surface functionalization of cotton cellulose with glycidyl methacrylate and its application for the adsorption of aromatic pollutants from wastewaters. *J. Hazard. Mater*. 170, 798–808. doi: 10.1016/j.jhazmat.2009.05.042

Watanabe, K., Tabuchi, M., Morinaga, Y., and Yoshinaga, F. (1998). Structural features and properties of bacterial cellulose produced in agitated culture. *Cellulose* 5, 187–200. doi: 10.1023/A:1009272904582

Wu, C. N., and Cheng, K. C. (2017). Strong, thermal-stable, flexible, and transparent films by self-assembled TEMPO-oxidized bacterial cellulose nanofibers. *Cellulose* 24, 269–283. doi: 10.1007/s10570-016-1114-8

Yang, R., Xu, S., Wang, Z., and Yang, W. (2005). Aqueous extraction of corncob xylan and production of xylooligosaccharides. LWT 38, 677–682. doi: 10.1016/j.lwt.2004.07.023

Zheng, A., Jiang, L., Zhao, Z., Huang, Z., Zhao, K., Wei, G., et al. (2015). Impact of torrefaction on chemical structure and catalytic fast pyrolysis behavior of hemicellulose, lignin and cellulose. *Energy Fuels* 29, 8027–8034. doi: 10.1021/acs.energyfuels.5b01765